Chapter 9
Optimization with Fluid-structure Interactions

Many applications involve inverse problems. A typical optimization problem could be the control of an inflow to reduce the vorticity or to stabilize the dynamics of a fluid-structure interaction problem. A related problem is the identification of parameters like Lamé coefficients by indirect measurements.

In this section, some basic principles for the optimization with partial differential equations and the application to simple, stationary fluid-structure interaction problems will be collected. For an intensive introduction to optimization and parameter identification with partial differential equations, we refer to the literature [191, 238, 325, 326]. On optimization with fluid-structure interactions, there is only little literature [79, 80, 134, 286]. From the large variety of different optimization techniques, we solely consider gradient based methods. The contents of this section have mainly been taken from [286], a collaboration with Thomas Wick.

A first thorough analysis of optimization problems with fluid-structure interactions is given by Failer [133, 134]. He also discusses the much more difficult and relevant case of non-stationary problems.

For gradient based optimization of coupled problems, it is necessary to assemble gradients of the fully coupled model. The adjoint solutions, based on these gradients, are sensitivities that indicate the impact of the control on the target functional. In partitioned methods, where the coupling is realized by an iterative algorithm only, this is a very difficult step. The sensitivities of fluid and solid problems alone are well studies. A proper inclusion of the coupling is a more difficult process. The correct transportation of adjoint information across the interface however will be essential.

T. Richter, *Fluid-structure Interactions*, Lecture Notes in Computational Science and Engineering 118, DOI 10.1007/978-3-319-63970-3_9

9.1 The Optimization Problem

We consider optimization problems, where the optimal solution is constraint to a stationary fluid-structure interaction problem. For simplicity, we will consider the ALE formulation from Chap. 5 only, such that $\mathbf{U} \in \mathbf{U}^D + \mathcal{X}$ is constraint to

$$\begin{aligned} A(\mathbf{U})(\Phi) = &\left(\rho_f J \left(\nabla \mathbf{v} \mathbf{F}^{-1} \mathbf{v}\right), \phi\right)_{\mathcal{F}} + \left(J \boldsymbol{\sigma}_f \mathbf{F}^{-T}, \nabla \phi\right)_{\mathcal{F}} - (J \rho_f \mathbf{f}, \phi)_{\mathcal{F}} \\ &+ \left(J \mathbf{F}^{-1} : \nabla \mathbf{v}^T, \xi\right)_{\mathcal{F}} + (\mathbf{F} \boldsymbol{\Sigma}_s, \nabla \phi)_{\mathcal{S}}, \end{aligned} \tag{9.1}$$

where $\mathbf{U}^D$ is an extension of the Dirichlet data and where $\mathbf{U} = \{\mathbf{v}, \mathbf{u}, p\}$ is found in

$$\mathcal{X} = H_0^1(\mathcal{F}; \Gamma_f^D)^d \times H_0^1(\mathcal{F} \cup \mathcal{I} \cup \mathcal{S}; \Gamma^D)^d \times L_0^2(\mathcal{F}).$$

We consider the following setting: by $K : \mathcal{X} \to \mathbb{R}$ we denote a given functional of interest. One example could be the outflow rate at a boundary part Γ_f^{out}

$$K_{\text{out}}(\mathbf{U}) = \int_{\Gamma_f^{\text{out}}} (\mathbf{v} \cdot \mathbf{n})^2 \, \mathrm{d}o, \tag{9.2}$$

or a functional of pointwise tracking type measuring the deflection of the solid

$$K_A(\mathbf{U}) = |\mathbf{u}(A) - \mathbf{u}^A|^2, \tag{9.3}$$

where $A \in \bar{\mathcal{S}}$ is a point within the solid, $\mathbf{u}^A \in \mathbb{R}^d$ a prescribed deflection. Regarding the discussion in Sect. 8.1.1.1, such a functional of point-type must be regularized to fit into the theoretical framework. In any case we assume that $K(\cdot)$ is two times Fréchet differentiable.

Furthermore, by $\mathbf{q} \in \mathbf{Q}_d$, we denote the control, coming from the control space $\mathbf{Q}_d$. Typical examples of controls could be the Lamé coefficients $\mathbf{q} = (\mu_s, \lambda_s)$, a two-dimensional control space $\mathbf{Q}_d \subset \mathbb{R}^2$, the inflow profile $\mathbf{q} = \mathbf{v}^{\text{in}}$, where $\mathbf{Q}_d = H^{1/2}(\Gamma_f^{\text{in}})$, a mean inflow pressure $\mathbf{q} = P^{\text{in}}$, where $\mathbf{Q}_d = \mathbb{R}$. Often, such controls are constrained, e.g. by allowing only for positive pressures up to a certain limit or by requiring the Lamé coefficients to satisfy some physical relations, i.e.

$$\mathbf{Q}_d = \{(\mu, \lambda) \in \mathbb{R}^2, \ \mu > 0\}.$$

In this study, we do not consider any control constraints.

The control $\mathbf{q}$ can enter the problem in various ways. We introduce the modified variational formulation

$$\mathbf{U} \in \mathbf{U}^D + \mathcal{X} : \quad A(\mathbf{q}, \mathbf{U})(\Phi) := A(\mathbf{U})(\Phi) + B(\mathbf{q}, \mathbf{U})(\Phi) = F(\Phi) \quad \forall \Phi \in \mathcal{X},$$

where by $B(\cdot,\cdot)(\cdot)$ we denote the *control form*. We specify this control form for two examples: First, we consider the case of controlling the average inflow pressure on the boundary Γ_f^{in}. We do not prescribe Dirichlet conditions for $\mathbf{v}$ on Γ_f^{IN} and use the trial space

$$\mathbf{v} \in \mathbf{v}^D + H_0^1(\mathcal{F}; \Gamma_f^D \setminus \Gamma_f^{\text{in}})^d,$$

such that natural Neumann conditions act. Together with

$$B(\mathbf{q},\mathbf{U})(\Phi) = -\langle \rho_f \nu_f J \nabla \mathbf{v}^T \mathbf{F}^{-T} \mathbf{F}^{-T} \mathbf{n}, \phi \rangle_{\Gamma_f^{\text{in}}} - \langle \mathbf{q} J \mathbf{F}^{-T} \mathbf{n}, \phi \rangle_{\Gamma_f^{\text{in}}}, \tag{9.4}$$

integration by parts reveals on Γ_f^{in} the condition

$$\rho_f \nu_f J \mathbf{F}^{-1} \nabla \mathbf{v} \mathbf{F}^{-T} \mathbf{n} - p J \mathbf{F}^{-T} \mathbf{n} = \mathbf{q} J \mathbf{F}^{-T} \mathbf{n},$$

which corresponds to an average inflow pressure of $\mathbf{q}$, see Sect. 2.4.2. Second, we consider the control of the parameter μ_s in the material law by introducing the control form

$$B(\mathbf{q},\mathbf{U})(\Phi) = (\mathbf{F}\boldsymbol{\Sigma}_s(\mathbf{q}) - \mathbf{F}\boldsymbol{\Sigma}_s(\mu_s^0), \nabla\phi)_{\mathcal{S}}, \tag{9.5}$$

where (for the St. Venant Kirchhoff material)

$$\boldsymbol{\Sigma}_s(\mathbf{q}) := 2\mathbf{q}\mathbf{E}_s + \lambda_s \operatorname{tr}(\mathbf{E}_s) I, \quad \mathbf{E}_s := \frac{1}{2}(\mathbf{F}^T\mathbf{F} - I). \tag{9.6}$$

By μ_s^0 we denote an initial guess. The goal of our optimization problem is to determine the optimal parameters $\mathbf{q} \in \mathbf{Q}_d$ such that the functional of interest $K(\cdot)$ gets minimal. This quantity of interest is completed by a regularization term of Tikhonov type, which involves a regularization parameter $\alpha > 0$

$$K(\mathbf{q},\mathbf{U}) := K(\mathbf{U}) + \frac{\alpha}{2} ||\mathbf{q} - \bar{\mathbf{q}}||_Q^2, \tag{9.7}$$

with a reference control $\bar{\mathbf{q}} \in \mathbf{Q}_d$ and a suitable norm $||\cdot||_Q$ in the control-space. With these preparations we can formulate the constrained optimization problem:

Problem 9.1 (Constrained Optimization Problem) *Find* $\mathbf{U} \in \mathbf{U}^D + \mathcal{X}$ *and* $\mathbf{q} \in \mathbf{Q}_d$, *such that*

$$K(\mathbf{q},\mathbf{U}) \to \min, \text{ where } A(\mathbf{q},\mathbf{U})(\Phi) = F(\Phi) \quad \forall \Phi \in \mathcal{X}.$$

Introducing the Lagrangian

$$L(\mathbf{q},\mathbf{U},\mathbf{Z}) = K(\mathbf{q},\mathbf{U}) + F(\mathbf{Z}) - \mathbf{A}(\mathbf{q},\mathbf{U})(\mathbf{Z}),$$

a minimum to Problem 9.1 must satisfy the first order optimality condition

$$L'(\mathbf{q},\mathbf{U},\mathbf{Z})(\delta\mathbf{q},\delta\mathbf{U},\delta\mathbf{Z}) = 0 \quad \forall\delta\mathbf{q}\in\mathbf{Q}_d,\ \forall\delta\mathbf{U}\in\mathcal{X},\ \forall\delta\mathbf{Z}\in\mathcal{X},$$

which corresponds to the following system of equations, the *Karush-Kuhn-Tucker conditions* (KKT):

$$\begin{aligned} A(\mathbf{q},\mathbf{U})(\Phi) &= F(\Phi) && \forall\Phi\in\mathcal{X},\\ A'_{\mathbf{U}}(\mathbf{q},\mathbf{U})(\Phi,\mathbf{Z}) &= K'_{\mathbf{U}}(\mathbf{q},\mathbf{U})(\Phi) && \forall\Phi\in\mathcal{X},\\ A'_{\mathbf{q}}(\mathbf{q},\mathbf{U})(\chi,\mathbf{Z}) &= K'_{\mathbf{q}}(\mathbf{q},\mathbf{U})(\chi) && \forall\chi\in\mathbf{Q}_d. \end{aligned} \tag{9.8}$$

The first equation is called the *state equation*, second the *adjoint equation* and the last one the *gradient equation*.

The adjoint equation is exactly the equation for the adjoint problem in the context of the *Dual Weighted Residual method* that has been introduced in Sect. 8.1.1 and which is detailed in (8.44). The specific form of the gradient equation strongly depends on the way that the control enters the problem. In the case of pressure control on the inflow boundary (9.4), this gradient equation reads

$$-\chi\langle J\mathbf{F}^{-T}\mathbf{n},\mathbf{z}\rangle_{\Gamma_f^{\text{in}}} = \chi\alpha(\mathbf{q}-\bar{\mathbf{q}}) \quad \forall\chi\in\mathbb{R}. \tag{9.9}$$

This allows to express the control $\mathbf{q}$ in terms of the other variables

$$\mathbf{q} = \bar{\mathbf{q}} - \frac{1}{\alpha}\langle J\mathbf{F}^{-T}\mathbf{n},\mathbf{z}\rangle_{\Gamma_f^{\text{in}}}, \tag{9.10}$$

which reduces the KKT system (9.8) to a coupled system of the state and the adjoint equation. Regarding the identification of the Lamé coefficient (9.5), the gradient equation gets

$$\chi\big(2\mathbf{F}\mathbf{E}_s,\nabla\mathbf{z}\big)_{\mathcal{S}} = \chi\alpha(\mathbf{q}-\bar{\mathbf{q}}) \quad \forall\chi\in\mathbb{R}, \tag{9.11}$$

where we directly computed the derivative of $\mathbf{\Sigma}_s(\mathbf{q})$ in direction of $\mathbf{q}$, compare (9.6). Again, we can explicitly compute the control $\mathbf{q}\in\mathbb{R}$ from this equation

$$\mathbf{q} = \bar{\mathbf{q}} + \frac{2}{\alpha}(2\mathbf{F}\mathbf{E}_s,\nabla\mathbf{z})_{\mathcal{S}}. \tag{9.12}$$

9.2 Reduced Formulation of the Optimization Problem

One possibility to solve the optimization problem is to approximate the KKT system (9.8). This however is a very large coupled system of equations involving prima problem, adjoint and control. Even if an explicit formula for the computation

of the control $\mathbf{q}$ can be used, a coupled problem in $\{\mathbf{U}, \mathbf{Z}\} \in \mathcal{X} \times \mathcal{X}$ remains to be solved. In terms of fluid-structure interaction, this refers to a coupled system of 10 (in 2d) and 14 (in 3d) equations. Instead, we first introduce a *reduced formulation* of the optimization, see problem [47, 191, 238, 325, 326] and [133, 134, 286] in the context of fsi.

Problem 9.2 (Unconstrained Optimization Problem) *Find* $\mathbf{q} \in \mathbf{Q}_d$*, such that*

$$k(\mathbf{q}) := K(\mathbf{q}, S(\mathbf{q})) \to \min, \tag{9.13}$$

where the solution operator $S : \mathbf{Q}_d \to \mathcal{X}$ *is defined as*

$$A(\mathbf{q}, S(\mathbf{q}))(\Phi) = F(\Phi) \quad \forall \Phi \in \mathcal{X}.$$

The solution of this unconstrained optimization problem is characterized by the first order necessary condition

$$k'(\mathbf{q})(\chi) = 0 \quad \forall \chi \in \mathbf{Q}_d, \tag{9.14}$$

a local minimum is guaranteed by the second-order optimality condition

$$k''(\mathbf{q})(\chi, \chi) \geq 0 \quad \forall \chi \in \mathbf{Q}_d.$$

To approximate the solutions of (9.14), we employ a Newton's method. Starting with $\mathbf{q}^0 \in \mathbf{Q}_d$ (one possibility is $\mathbf{q}^0 = \bar{\mathbf{q}}$) we iterate

$$k''(\mathbf{q}^l)(\delta\mathbf{q}^l, \chi) = -k'(\mathbf{q}^l)(\chi) \quad \forall \chi \in \mathbf{Q}_d, \quad \mathbf{q}^{l+1} = \mathbf{q}^l + \omega^l \delta\mathbf{q}^l,$$

where $\omega^l \in \mathbb{R}$ is a possible relaxation parameter. Every step of this Newton loop requires the evaluation of the residual and the solution of the Hessian. As the solution $\mathbf{U} = S(\mathbf{q})$ is implicitly given, this involves some effort.

Lemma 9.3 (Residual of the Newton Iteration) *Let* $\mathbf{q}^l \in \mathbf{Q}$ *be given. Then, the residual is given by*

$$-k'(\mathbf{q}^l)(\chi) := -\alpha(\mathbf{q}^l - \bar{\mathbf{q}}, \chi) + A'_{\mathbf{q}}(\mathbf{q}^l, \mathbf{U}^l)(\chi, \mathbf{Z}^l),$$

where the solution $\mathbf{U}^l \in \mathcal{X}$ *and the adjoint solution* $\mathbf{Z}^l \in \mathcal{X}$ *are given by*

$$\begin{aligned} &(1) && A(\mathbf{q}^l, \mathbf{U}^l)(\Phi) = F(\Phi) && \forall \Phi \in \mathcal{X}, \\ &(2) && A'_U(\mathbf{q}^l, \mathbf{U}^l)(\Phi, \mathbf{Z}^l) = K'_{\mathbf{U}}(\mathbf{q}^l, \mathbf{U}^l)(\Phi) && \forall \Phi \in \mathcal{X}. \end{aligned}$$

Proof Let $\mathbf{U}^l = S(\mathbf{q}^l)$ be the solution to (1) and $\mathbf{Z}^l \in \mathcal{X}$ be the solution to (2). Then, formal derivation of $k(\mathbf{q})$ yields

$$k'(\mathbf{q}^l)(\chi) = K'_{\mathbf{q}}(\mathbf{q}^l, S(\mathbf{q}^l)) + K'_{\mathbf{U}}(\mathbf{q}^l, S(\mathbf{q}^l))(S'(\mathbf{q}^l)\chi).$$

Deriving the state equation to $\mathbf{q}$ gives a relation for $S'(\mathbf{q}^l)\chi$

$$A'_q(\mathbf{q}^l, S(\mathbf{q}^l))(\Phi) = -A'_{\mathbf{U}}(\mathbf{q}^l, S(\mathbf{q}^l))(S'(\mathbf{q}^l)\chi, \Phi) \quad \forall \Phi \in \mathcal{X}. \tag{9.15}$$

Then, by using (9.7), the adjoint equation and this relation (9.15)

$$\begin{aligned} k'(\mathbf{q}^l)(\chi) &= \alpha(\mathbf{q} - \bar{\mathbf{q}}, \chi)_{\mathbf{Q}} + A'_{\mathbf{U}}(\mathbf{q}^l, S(\mathbf{q}^l))(S'(\mathbf{q}^l)\chi, \mathbf{Z}^l) \\ &= \alpha(\mathbf{q} - \bar{\mathbf{q}}, \chi)_{\mathbf{Q}} - A'_q(\mathbf{q}^l, S(\mathbf{q}^l))(\mathbf{Z}^l). \end{aligned}$$

□

For estimation of the residual, we must first solve the *state equation*, followed by a solution of the *adjoint equation*. These equations can be solved independently. Once the residual is given, the Hessian equation must be solved.

Lemma 9.4 (Hessian of the Newton Iteration) *Let $\mathbf{q}^l \in \mathbf{Q}$ be given, $\mathbf{U}^l$ and $\mathbf{Z}^l$ be the adjoint solutions defined in Lemma 9.3. Let $\{\chi_1, \ldots, \chi_{\#q}\}$ be a basis of $\mathbf{Q}$. Then, solve the $\#q$* tangent equations *and* adjoint for Hessian equations *for $\mathbf{U}^l_1, \ldots, \mathbf{U}^l_{\#q}$ and $\mathbf{Z}^l_1, \ldots, \mathbf{Z}^l_{\#q}$*

$$\begin{aligned} &i = 1, \ldots, \#q: \\ &A'_{\mathbf{U}}(\mathbf{q}^l, \mathbf{U}^l)(\mathbf{U}^l_i, \Phi) = -A'_{\mathbf{q}}(\mathbf{q}^l, \mathbf{U}^l)(\chi_i, \Phi) \qquad \forall \Phi \in \mathcal{X} \\ &A'_{\mathbf{U}}(\mathbf{q}^l, \mathbf{U}^l)(\Phi, \mathbf{Z}^l_i) = K''_{\mathbf{UU}}(\mathbf{q}^l, \mathbf{U}^l)(\mathbf{U}^l_i, \Phi) \\ &\qquad\qquad - A''_{\mathbf{qU}}(\mathbf{q}^l, \mathbf{U}^l)(\chi_i, \Phi, \mathbf{Z}^l) \\ &\qquad\qquad - A''_{\mathbf{UU}}(\mathbf{q}^l, \mathbf{U}^l)(\mathbf{U}^l_i, \Phi, \mathbf{Z}^l) \quad \forall \Phi \in \mathcal{X}. \end{aligned} \tag{9.16}$$

Then, the Hessian (in the Basis $\{\chi_i\}$) is given as

$$\begin{aligned} \mathbf{k}_{ij}(\mathbf{q}^l) := \alpha(\chi_i, \chi_j)_{\mathbf{Q}} &- A''_{\mathbf{qq}}(\mathbf{q}^l, \mathbf{U}^l)(\chi_i, \chi_j, \mathbf{Z}^l) \\ &- A''_{\mathbf{qU}}(\mathbf{q}^l, \mathbf{U}^l)(\chi_i, \mathbf{U}^l_j, \mathbf{Z}^l) - A'_{\mathbf{q}}(\mathbf{q}^l, \mathbf{U}^l)(\chi_i, \mathbf{Z}^l_j). \end{aligned}$$

Proof Derivation of the residual gives

$$\begin{aligned} k''(\mathbf{q}^l)(\chi, \tau) = \alpha(\chi, \tau)_{\mathbf{Q}} &- A''_{\mathbf{qq}}(\mathbf{q}^l, \mathbf{U}^l)(\chi, \tau, \mathbf{Z}^l) \\ &- A''_{\mathbf{qU}}(\mathbf{q}^l, \mathbf{U}^l)(\chi, S'(\mathbf{q}^l)\tau, \mathbf{Z}^l) - A'_{\mathbf{q}}(\mathbf{q}^l, \mathbf{U}^l)(\chi, Z'(\mathbf{q})\tau). \end{aligned} \tag{9.17}$$

The first two terms can be evaluated with the knowledge of $\mathbf{q}^l, \mathbf{U}^l$ and $\mathbf{Z}^l$. By derivation of the state equation we obtain the *tangent equation* which we solve for $\mathbf{U}^l_\tau := S'(\mathbf{q}^l)\tau$

$$A'_{\mathbf{U}}(\mathbf{q}^l, \mathbf{U}^l)(\mathbf{U}^l_\tau, \Phi) = -A'_{\mathbf{q}}(\mathbf{q}^l, \mathbf{U}^l)(\tau, \Phi) \quad \forall \Phi \in \mathcal{X}.$$

This allows to evaluate the third term $A''_{\mathbf{qu}}$ in (9.17). For evaluation of the last term we solve for $\mathbf{Z}^l_\tau = Z'(\mathbf{q}^l)\tau$ given by the derivative of the adjoint equation

$$\begin{aligned} A'_U(\mathbf{q}^l, \mathbf{U}^l)(\Phi, \mathbf{Z}^l_\tau) = K''_{\mathbf{UU}}(\mathbf{q}^l, \mathbf{U}^l)(\mathbf{U}^l_\tau, \Phi) \\ - A''_{\mathbf{qU}}(\mathbf{q}^l, \mathbf{U}^l)(\tau, \Phi, \mathbf{Z}^l) - A''_{\mathbf{UU}}(\mathbf{q}^l, \mathbf{U}^l)(\mathbf{U}^l_\tau, \Phi, \mathbf{Z}^l). \end{aligned}$$

□

Compared to the residual evaluation, the assembly of the Hessian calls for the additional effort of solving *#q tangent equations* and *#q adjoint for Hessian equations*. Each of these problems is linear and has the same dimension as the adjoint problem. The overall effort appears to be rather large, by using the reduced solution approach, one however circumvents the introduction of large systems, where state and adjoint solution are coupled. For the discussed examples with a one-dimensional control space $\mathbf{Q}_d$, one Newton iteration requires the solution of the nonlinear state equation, the solution of one linear adjoint, one *tangent* and one *adjoint for Hessian equation*.

9.3 Realization with Fluid-structure Interactions

The described Newton iteration for the optimization problem requires the evaluation of several further derivatives of the variational formulation. We have already derived the Jacobian in Sect. 5.2.2, which is the system matrix of the tangent equation (9.16). Its inverse is the system matrix of the adjoint equation and further the system matrix of the *adjoint for Hessian equation*, also shown in (9.16). All the remaining derivatives are required for different right hand sides of the problems. Their evaluation is partially simple, e.g. $A'_{\mathbf{q}}$, $K''_{\mathbf{UU}}$ or $A''_{\mathbf{qU}}$. Only the second derivative of $A(\cdot)(\cdot)$ with respect to the solution $\mathbf{U}$ will give rise to excessive terms due to the ALE mapping. Here, given $\mathbf{U}^l_i$ we propose the approximation by finite differences

$$A''_{\mathbf{UU}}(\mathbf{q}^l, \mathbf{U}^l)(\mathbf{U}^l_i, \Phi, \mathbf{Z}^l) \approx \frac{A'_{\mathbf{U}}(\mathbf{q}^l, \mathbf{U}^l + \varepsilon \mathbf{U}^l_i)(\Phi, \mathbf{Z}^l) - A'_{\mathbf{U}}(\mathbf{q}^l, \mathbf{U}^l)(\Phi, \mathbf{Z}^l)}{\varepsilon},$$

where $\varepsilon > 0$ is a parameter that has to be carefully chosen, compare the discussion in Sect. 5.2.3 and Fig. 5.8.

9.4 Parameter Identification Test

Based on the benchmark problem fsi-1 by Hron and Turek [199], see also Sect. 6.6, we formulate a parameter identification test case. According to [329, 330], the geometry has been changed by slightly widening the beam to $h = 0.04$ instead of $h = 0.02$ in the original problem, compare Fig. 9.1.

We initially "forget" the Lamé coefficient μ_s and try to reconstruct it based on a measurement of the deformation of the beam in the point $A = (0.6, 0.2)$. We introduce the regularized cost functional

$$K(\mathbf{q}, \mathbf{U}) = |\mathbf{u}_y(A) - \mathbf{u}_y^{\text{ref}}|^2 + \frac{\alpha}{2}|\mathbf{q} - \bar{\mu}|^2,$$

where $\bar{\mu} \in \mathbb{R}$ is an initial guess and $\alpha = 10^{-3}$ the Tikhonov parameter. The control $\mathbf{q} \in \mathbb{R}$ enters in form of a material parameter, such that the control form is given by (9.5).

The flow is driven by a parabolic inflow profile on Γ_{in} with maximum velocity $\bar{\mathbf{v}}^{\text{in}} = 1.5$ m/s and the remaining parameters used in this test case are given by

$$\rho_f = \rho_s = 10^3 \frac{kg}{m^3}, \quad \nu_f = 10^{-3} \frac{m^2}{s}, \quad \nu_s = 0.4.$$

On the outflow boundary Γ_f^{out} we prescribe the *do-nothing* outflow condition, see Sect. 2.4.2. All computations in this sections have been carried out by Thomas Wick [286, 347] using the software library deal.II [24].

In Table 9.1 we determine the deformation $\mathbf{u}_y(A)$ in the tip of the beam considering the Lamé coefficient $\mu^{\text{ref}} = 500{,}000$ on a sequence of two meshes in forward simulations. These values act as reference values $\mathbf{u}_y^{\text{ref}}$ for each optimization test case.

We start the actual optimization loop with the initial control $\mathbf{q}^0 = 5000$ far away from the optimal state $\mathbf{q}^{\text{opt}} = \mu^{\text{opt}} = 500{,}000$. In Table 9.2 we indicate the results of the optimization algorithm on two meshes, using the corresponding reference deformation $\mathbf{u}_y^{\text{ref}}(A)$ on each level. Here, it shows, that the presented

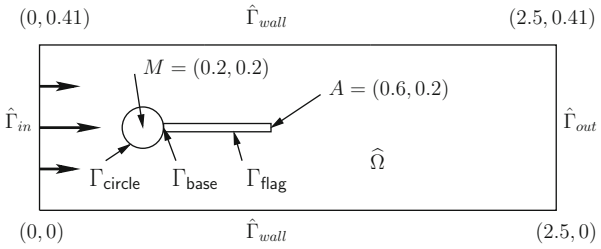

Fig. 9.1 Configuration of the parameter identification test case with the modified fsi-1 benchmark configuration. The thickness of the beam is increased to 0.04 (from 0.02 in the standard fsi benchmark problem)

Table 9.1 Forward computation for obtaining reference values $\mathbf{u}^{\text{ref}}(A)$ using the exact Lamé coefficient $\mu^{\text{opt}} = 500{,}000$ on two subsequent meshes

DoF	μ^{ref}	$\mathbf{u}_y^{\text{ref}}$
19,488	500,000	$8.2747 \cdot 10^{-4}$
76,672	500,000	$8.2289 \cdot 10^{-4}$

Table 9.2 *Modified fsi-1* parameter estimation problem

Step	μ	$\mathbf{u}_y(A)$	$\lvert\mathbf{u}_y(A) - \mathbf{u}_y^{\text{ref}}\rvert$	Residual
(a) Results on a mesh with 19,488 unknowns, $\mathbf{u}_y^{\text{ref}} = 0.00082747$				
1	5000	$2.0118 \cdot 10^{-3}$	$1.18 \cdot 10^{-3}$	$1.00 \cdot 10^{-0}$
2	188,133	$1.1992 \cdot 10^{-3}$	$3.72 \cdot 10^{-4}$	$5.90 \cdot 10^{-1}$
3	498,310	$8.2884 \cdot 10^{-4}$	$1.37 \cdot 10^{-6}$	$2.76 \cdot 10^{-3}$
4	499,767	$8.2770 \cdot 10^{-4}$	$2.30 \cdot 10^{-7}$	$4.01 \cdot 10^{-6}$
5	499,769	$8.2768 \cdot 10^{-4}$	$2.10 \cdot 10^{-7}$	$6.58 \cdot 10^{-9}$
(b) Results on a mesh with 76,672 unknowns, $\mathbf{u}_y^{\text{ref}} = 0.00082289$				
1	5000	$2.000 \cdot 10^{-3}$	$1.18 \cdot 10^{-3}$	$1.00 \cdot 10^{-0}$
2	118,309	$1.347 \cdot 10^{-3}$	$5.24 \cdot 10^{-4}$	$7.23 \cdot 10^{-1}$
3	493,626	$8.279 \cdot 10^{-4}$	$5.01 \cdot 10^{-6}$	$1.16 \cdot 10^{-2}$
4	499,756	$8.232 \cdot 10^{-4}$	$3.10 \cdot 10^{-7}$	$2.27 \cdot 10^{-5}$
5	499,768	$8.231 \cdot 10^{-4}$	$2.10 \cdot 10^{-7}$	$2.70 \cdot 10^{-8}$

Results of the optimization loop for two different meshes, using the reference values as collected in Table 9.1. Showing iteration, control $\mathbf{q}^l = \mu^l$, deformation $\mathbf{u}_y(A)$, absolute error in deformation and Newton residual

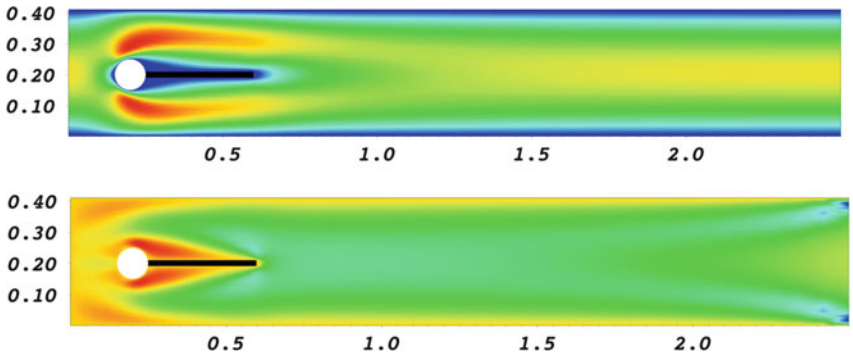

Fig. 9.2 *Modified fsi-1* parameter estimation: x-velocity profile $\mathbf{v}_x$ (*top*) and corresponding adjoint solution $\mathbf{z}_x$ (*bottom*)

Newton optimization scheme with the exactly derived adjoint problems for the monolithic variational formulation yields a very efficient (quadratic) convergence to the optimal state.

In Fig. 9.2, we show plots of *x*-velocity and the corresponding adjoint solution component for the solution of this optimization problem.

9.5 Optimal Control Test

As second problem we consider an optimal control test. Figure 9.3 shows the configuration. By controlling the inflow pressure on Γ_f^{in} by $p_f^{\text{in}} \in \mathbb{R} = \mathbf{q}_f \in \mathbb{R}$ we aim at maximizing the outflow at Γ_f^{out}. An elastic obstacle $\mathcal{S}$ is embedded in the flow domain. At increased velocities, this obstacle will be sucked to the top of the domain and closes the channel, such that the flow rate will decrease again.

The problem is constructed such that the optimal solution can be easily verified by forward simulations to offer an easy test case for the optimization routines and in particular for the derivation of the adjoint formulations. Control is realized by the pressure control form (9.4), the target function is given by

$$K_{\text{out}}(\mathbf{q}, \mathbf{U}) = -\int_{\Gamma_f^{\text{out}}} (\mathbf{n} \cdot \mathbf{v})^2 \, \mathrm{d}s + \frac{\alpha}{2} |\mathbf{q} - \bar{\mathbf{q}}|^2, \tag{9.18}$$

where $\alpha > 0$ is the regularization parameter. We changed the sign to obtain a minimization problem. The material parameters are chosen as

$$\rho_f = \rho_s = 10^3 \,\mathrm{kg} \cdot \mathrm{m}^{-3}, \quad \nu_f = 10^{-3} \,\mathrm{m}^2 \cdot \mathrm{s}^{-1}, \quad \nu_s = 0.4, \quad \mu_s = 500 \,\mathrm{kg} \cdot \mathrm{m}^{-1} \mathrm{s}^{-1}.$$

Velocity and deformation as set to zero on all outer boundaries Γ_{wall}.

Figure 9.4 shows results of forward simulation for different values of the control $\mathbf{q}$, i.e. the average inflow pressure on Γ_f^{in}. Considering higher pressures, the beam will narrow the channel and reduce the outflow rate; we refer the reader to Fig. 9.5 for snapshots of the solution for different inflow pressures $\mathbf{q} = p_{\text{in}}$. From the forward simulation we estimate $\mathbf{q}^{\text{opt}} \in [0.23, 0.24]$.

This test case is very challenging as control and target functional are both living within the fluid. Without the interaction to the solid, no effect would take place. This example asks for a careful analysis of the adjoint information transport from the fluid to the solid and back to the fluid. In [286] we study this problem with an

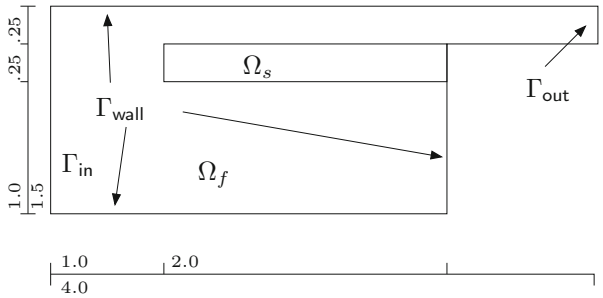

Fig. 9.3 Configuration of the optimal control test case. We control the inflow pressure on Γ_{in} with the goal to maximize the outflow rate on Γ_{out}

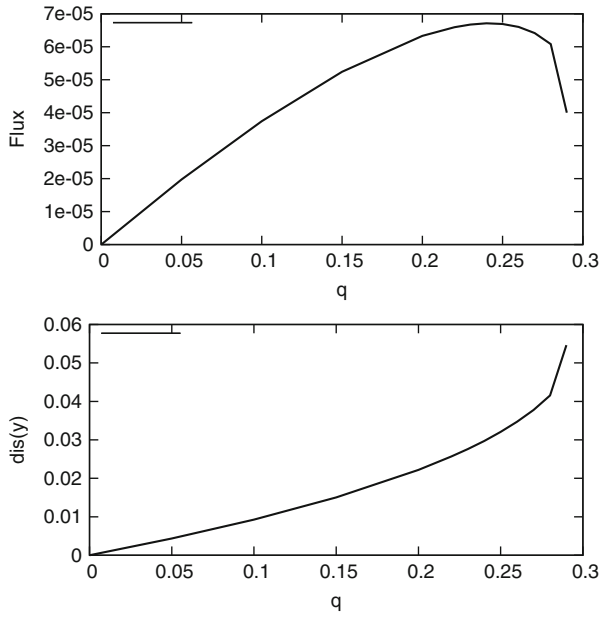

Fig. 9.4 Forward simulations for varying inflow pressures $\mathbf{q}$. In the *upper plot* we show the outflow rate $K_{\text{out}}(\mathbf{q}, \mathbf{U}(\mathbf{q}))$. In the *lower plot* we indicate the deformation of the tip of the beam $\mathbf{u}_y(A)$. The outflow rate decreases for $\mathbf{q} > 0.25$. We expect to find the optimal control close to this point

approximated adjoint that neglects the coupling conditions. It is shown that such an approximation does not carry sufficient information for efficiently solving the optimization problem.

To approximate this problem, we use an updated Tikhonov parameterization, where both the parameter α and the parameter $\bar{\mathbf{q}}$ in

$$K(\mathbf{q}, \mathbf{U}) = K_{\text{out}}(\mathbf{U}) + \frac{\alpha}{2}|\mathbf{q} - \bar{\mathbf{q}}|^2,$$

are updated. We start with $\bar{\mathbf{q}}^0 = \mathbf{q}^0 = 0.1$ and take the last available optimum in each step. Furthermore, the parameter α is reduced step by step. In Table 9.3, we show the convergence of this iterated Tikhonov scheme, together with the chosen values for α^i and the obtained controls p^i_{opt}. As expected by the forward computation, the maximal flux is reached for $p_{opt} \sim 0.23$–0.24. Indeed, it can be observed that the channel is narrowed in the maximized solution as illustrated in Fig. 9.5. Here, in the unloaded reference configuration, the gap has a width of 0.125. Using the initial control $\bar{p}^0_{\text{in}} = 0.1$, the gap is narrowed to 0.115 and in the optimum state, for $p_{\text{opt}} \approx 0.24$, the size of the gap is reduced to 0.095. This is an overall

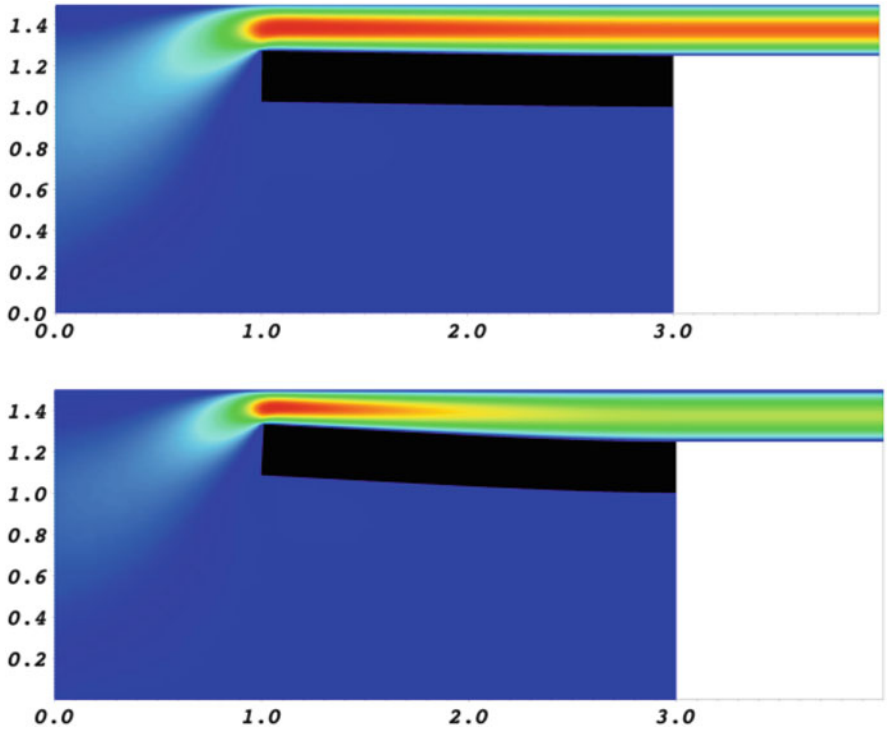

Fig. 9.5 Maximization of the outflow rate. At the *top* we show the velocity for the initial control $\mathbf{q}^0 = 0.1$ and in the *bottom* we show the solution close to the optimal control $\mathbf{q}^{\text{opt}} \approx 0.23$

Table 9.3 Maximizing the outflow rate $K_{\text{out}}(\mathbf{U})$ by controlling the inflow pressure $q = p_{\text{in}}$ on three globally refined meshes using an iterated Tikhonov regularization with Tikhonov parameter α and reference control $\bar{p}_{\text{in}}$

DoF	$\bar{p}_{\text{in}}$	α	$u_y(A)$	$K_{\text{out}}(U)$	p_{opt}
12,612	0.1000	$1.0 \cdot 10^{-5}$	$0.97 \cdot 10^{-2}$	$3.87 \cdot 10^{-5}$	0.1038
	0.1038	$7.5 \cdot 10^{-6}$	$1.02 \cdot 10^{-5}$	$4.04 \cdot 10^{-5}$	0.1090
	0.1090	$5.0 \cdot 10^{-6}$	$1.11 \cdot 10^{-5}$	$4.29 \cdot 10^{-5}$	0.1170
	0.1170	$2.5 \cdot 10^{-6}$	$1.30 \cdot 10^{-5}$	$4.78 \cdot 10^{-5}$	0.1335
	0.1335	$1.0 \cdot 10^{-6}$	$1.85 \cdot 10^{-5}$	$5.87 \cdot 10^{-5}$	0.1759
	0.1759	$7.5 \cdot 10^{-7}$	$2.43 \cdot 10^{-5}$	$6.53 \cdot 10^{-5}$	0.2254
	0.2254	$5.0 \cdot 10^{-7}$	$2.72 \cdot 10^{-5}$	$6.67 \cdot 10^{-5}$	0.2280
49,540	0.1759	$1.0 \cdot 10^{-6}$	$2.46 \cdot 10^{-5}$	$6.52 \cdot 10^{-5}$	0.2135
	0.2135	$7.5 \cdot 10^{-7}$	$2.84 \cdot 10^{-5}$	$6.70 \cdot 10^{-5}$	0.2330
196,356	0.1759	$1.0 \cdot 10^{-6}$	$2.42 \cdot 10^{-5}$	$6.50 \cdot 10^{-5}$	0.2111
	0.2111	$7.5 \cdot 10^{-7}$	$2.92 \cdot 10^{-5}$	$6.71 \cdot 10^{-5}$	0.2367

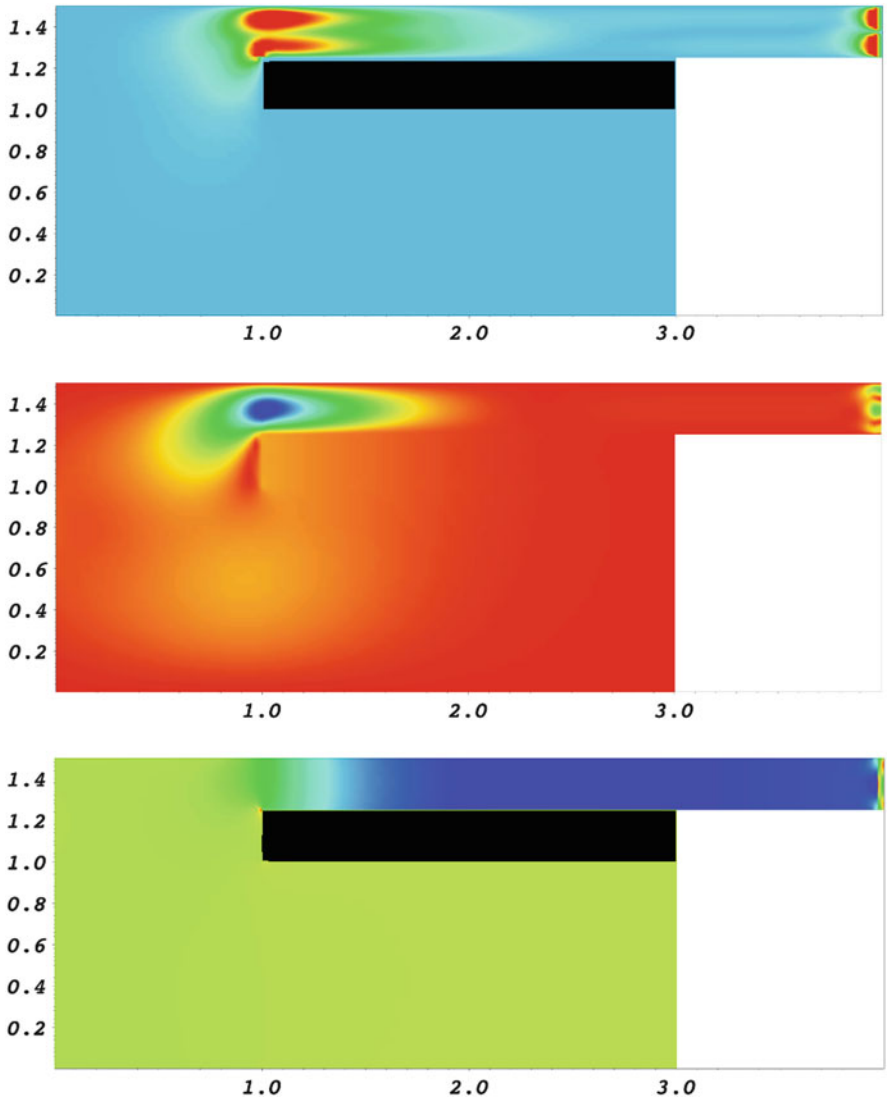

Fig. 9.6 Maximization of the outflow rate. Adjoint solution with respect to the velocity (*top*), displacement (*middle*) and pressure (*bottom*). All solutions are displaced in the undeformed reference configuration in ALE coordinates

reduction of about 25%. Finally, Fig. 9.6 illustrates the three components $\mathbf{z}_v, z_p, \mathbf{z}_n$ of the adjoint solution.

We finally note that we expect different results, if this problem would be treated with a fully non-stationary approach. At very high pressures one has to expect instabilities that will cause a flattering of the elastic obstacle and that might finally prevent the full closure of the channel.